Energetics of Diphtheria Toxin Membrane Insertion and Translocation: Calorimetric Characterization of the Acid pH Induced Transition†

Glen Ramsay, Diana Montgomery, Dolores Berger, and Ernesto Freire*

Department of Biology, The Johns Hopkins University, Baltimore, Maryland 21218

Received June 15, 1988; Revised Manuscript Received August 31, 1988

ABSTRACT: The pH and temperature stabilities of diphtheria toxin and its fragments have been studied by high-sensitivity differential scanning calorimetry. These studies demonstrate that the pH-induced conformational transition associated with the mechanism of membrane insertion and translocation of the toxin involves a massive unfolding of the toxin molecule. At physiological temperatures (37 °C), this process is centered at pH 4.7 at low ionic strength and at pH 5.4 in the presence of 0.2 M NaCl. At pH 8, the thermal unfolding of the nucleotide-bound toxin is centered at 58.2 °C whereas that of the nucleotide-free toxin is centered at 51.8 °C, indicating that nucleotide binding (ApUp) stabilizes the native conformation of the toxin. The unfolding profile of the toxin is consistent with two transitions most likely corresponding to the A fragment (T_m = 54.5 °C) and the B fragment (T_m = 58.4 °C), as inferred from experiments using the isolated A fragment. These two transitions are not independent, judging from the fact that the isolated A fragment unfolds at much lower temperatures (T_m = 44.2 °C) and that the B fragment is insoluble in aqueous solutions when separated from the A fragment. Interfragment association contributes an extra −2.6 kcal/mol to the free energy of stabilization of the A fragment. Whereas the unfolding of the entire toxin is irreversible, the unfolding of the A fragment is a reversible process. These findings provide a thermodynamic basis for the refolding of the A fragment after reexposure to neutral pH immediately following translocation across the lysosomal membrane.

Proteins which are capable of changing their water/membrane solubility in response to changes in the environment offer a unique experimental opportunity to study the events associated with the process of protein–membrane association and insertion. Proteins which are permanently membrane bound, as is the case with many integral membrane proteins, do not offer a convenient handle to dissect the forces and energies involved in such important events as protein binding, insertion, or translocation. Diphtheria toxin is an example of a protein which occurs in both water-soluble and membrane-associated states. It is secreted by *Corynebacterium diphtheriae* as a single peptide with a molecular weight of 58 342. After secretion this polypeptide is proteolytically nicked to yield fragments A (M_r = 21 100) and B (M_r = 37 200) which remain associated via a disulfide bond (DeLange et al., 1979; Drazin et al., 1979; Falmagne et al., 1985). When the interchain disulfide bond is reduced and the two fragments are dissociated, the free A fragment is capable of catalyzing the ADP-ribosylation and inactivation of elongation factor II (EF II), resulting in the inhibition of protein synthesis. Diphtheria toxin binds endogenous dinucleotides, particularly adenylyl-3′,5′-uridine 3′-monophosphate (ApUp) with high affinity (K_d = 1.8 × 10^{-9} at 37 °C) (Collins et al., 1984). Furthermore, it is capable of dimerization (Goor, 1968) and self-ribosylation (Gill & Steinhaus, 1974).

The initial step of cytotoxicity by diphtheria toxin is the binding of the toxin to a cell surface receptor. The identity of the receptor is unknown, but it is suspected to be a glycoprotein (Proia et al., 1979; Hranitzky et al., 1985; Cieplak et al., 1987). The toxin is then endocytosed, where it is exposed to a pH of approximately 5 (Ohkuma & Poole, 1978; Jensen & Bainton, 1973). The exposure of the toxin to an acidic environment is thought to provide the necessary driving force for the insertion of the toxin into the membrane and the translocation of the A fragment into the cytosol. There is evidence that following toxin insertion and translocation of the A fragment the disulfide bond is reduced on the cytosolic side of the membrane (Moskaug et al., 1987) and the A fragment is released into the cytosol. Lysosomotrophic drugs such as NH_4Cl or chloroquine (Draper & Simon, 1980; Marnell et al., 1984; Sandvig & Olsnes, 1980, 1981, 1982) inhibit the acidification of the endosome and block the cytotoxic effects of the toxin. Cells that have been treated with these drugs can still be intoxicated by brief exposure to a low pH, thus illustrating the necessity of endosome acidification for the translocation step. In vivo studies have shown that exposure of the toxin to a low pH triggers a conformational change which results in increased hydrophobicity of the toxin (Sandvig & Olsnes, 1981; Blewitt et al., 1984). The exact nature and extent of this change are still unknown.

In this paper we present a thermodynamic characterization of the thermal and pH stabilities of diphtheria toxin. These studies were performed by high-sensitivity differential scanning calorimetry and have allowed us to develop the pH/temperature stability diagram of the toxin. These studies have permitted us to evaluate the energetics and magnitude of the pH-induced transition and to dissect the individual contributions to the overall stability by each of the toxin fragments. These studies provide a thermodynamic basis to the molecular events underlying the mechanism of toxin membrane insertion and translocation.

Materials and Methods

Toxin Purification. Crude diphtheria toxin (lot D608) was purchased from Connaught Laboratories Ltd., Willowdale, Canada. The crude toxin was dialyzed three times against 4 L of 50 mM Tricine (Sigma), pH 7.2 (Tricine buffer), at

†This work has been supported by a grant from the National Institutes of Health (GM-37911).

0006-2960/89/0428-0529$01.50/0

4 °C and purified essentially by the method given by Collier and Kandel (1971) with the following modifications for the utilization of HPLC. Dialyzed toxin was passed through a 0.22-μm membrane filter, loaded in 250-μL aliquots onto a TSK DEAE-5PW (LKB) ion-exchange column mounted on a LKB 2150 HPLC pump, and eluted with a linear gradient of 65–130 mM NaCl in Tricine buffer over a 26-min period at a flow rate of 0.5 mL/min. The elution profile was monitored by a LKB 2140 diode array detector. The toxin eluted as a single, large, asymmetric peak which was concentrated by dialyzing against three times the volume of saturated ammonium sulfate, pH 7.2. The precipitated protein was collected by centrifugation at 30000*g* in a Beckman J2-21 centrifuge with a JA-20 rotor for 30 min. The pellets were resuspended in Tricine buffer to approximately 10 mg/mL and dialyzed two times against 4 L of Tricine buffer. The solution was briefly centrifuged to remove particulates and then applied in 100-μL injections to a molecular sieve column (TSKgel G3000-SW, LKB) with 150 mM NaCl in Tricine buffer at flow rate of 0.75 mL/min. Fractions containing monomeric toxin were pooled and concentrated to 2 mg/mL by ammonium sulfate precipitation and dialyzed three times against 4 L Tricine buffer. Diphtheria toxin purified by this method yielded better than 90% pure nicked monomer. Impurities consisted mainly of unnicked toxin, and proteolytic fragments of toxin. The nicked monomer consisted of a native mixture of nucleotide-free and -bound toxin species. The relative amounts of nucleotide free and nucleotide bound varied from lot to lot but were in the range of 50%–90% nucleotide bound.

Separation of Nucleotide-Free and -Bound Toxin Species. After being dialyzed three times against 4 L of Tricine buffer, the crude toxin was passed through a 0.22-μm membrane filter and loaded onto a Matrex Green A (Amicon Corp., Lexington, MA) column (1.8 × 20 cm) at a flow rate of 0.07 mL/min. The column was rinsed with Tricine buffer until the nucleotide-bound toxin and impurities had passed through; then, Tricine buffer containing 0.75 M NaCl was used to elute the nucleotide-free toxin. The nucleotide-free and -bound fractions were pooled separately and concentrated by ammonium sulfate precipitation. The toxin species were resuspended and dialyzed, and monomeric toxin was obtained by molecular sieve chromatography as described for the purification of toxin containing a native mixture of species. The nucleotide-bound and -free species obtained were 99% pure nicked, monomeric toxin as judged by SDS gel electrophoresis.

Isolation of A Fragment. Diphtheria toxin A fragment was prepared essentially by the method of Kandel et al. (1974). A total of 3 mL of nucleotide-bound toxin (3 mg/mL) which had been purified as described above was allowed to react with 0.1 M dithiothreitol (DTT) in the presence of 0.5 M guanidine hydrochloride in Tricine buffer at 37 °C for 45 min. The reaction mixture was centrifuged at 27000*g* for 18 min. The supernatant was collected and dialyzed overnight against 50 volumes of 0.1 M 2-hydroxyethyl disulfide in Tricine buffer at 4 °C to block free sulfhydryl groups. The protein solution was concentrated to approximately 1 mL with a YM10 membrane filter in a 10-mL stirred ultrafiltration cell (Amicon) and passed over a Sephadex G-100 column at 4 °C equilibrated with 50 mM Tricine, pH 8.2. The fractions containing the A fragment were pooled and concentrated by ultracentrifugation to a total volume of 2 mL (0.5 mg/mL). The isolated A fragment prepared in this way was 94% pure as judged by SDS and native gel electrophoresis analysis.

Polyacrylamide Gel Electrophoresis. Toxin purity was checked by discontinuous sodium dodecyl sulfate (SDS)–polyacrylamide gel electrophoresis (PAGE) with a 3% stacking gel (pH 6.8) and a 10% running gel (pH 8.8). Samples were prepared by mixing 20 μL of protein with 20 μL of 17% sucrose, 0.17% phenol red, 1 M Tris (pH 8.8) (sucrose solution), 20 μL of 1.7 M urea, and 3% SDS (denaturing solution) (3% β-mercaptoethanol was included in the denaturing solution for reducing gels). This mixture was boiled for 2 min, and 55 μL was loaded onto the gel.

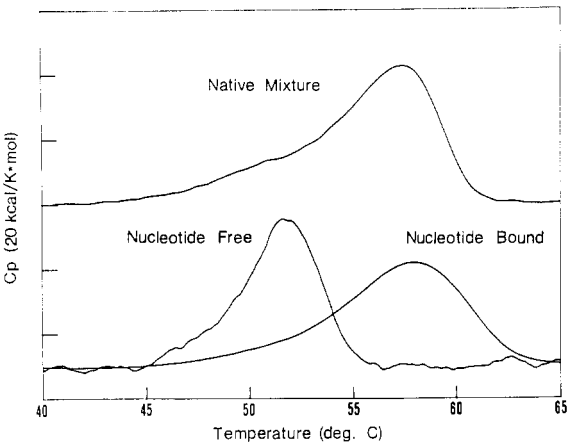

FIGURE 1: Excess heat capacity (C_p) vs temperature of nicked, monomeric diphtheria toxin, pH 8. The scan rates were 60 °C/h, and the protein concentrations were 1–2 mg/mL for nucleotide-bound toxin and 0.5 mg/mL for nucleotide-free toxin.

Native PAGE was used to check the dimer content and to partially resolve monomer toxin species by their charge differences. Native gels were prepared by the same protocol as for SDS–PAGE, except that water was substituted for concentrated SDS. The samples were prepared by mixing 20 μL of sample with 20 μL of sucrose solution; 35 μL was loaded onto the gel.

Differential Scanning Calorimetry. All calorimetric scans were performed on a Microcal MC-2 differential scanning calorimeter (DSC). The calorimetric unit was interfaced to an IBM PC microcomputer using an A/D converter board (Data Translation DT-2801) for automatic data collection and analysis. A scan rate of 60 °C/h was used, unless otherwise noted. Protein concentrations were determined after each scan (Lowry et al., 1951) and ranged between 1 and 2 mg/mL for nucleotide-bound toxin. The concentration of nucleotide-free toxin was 0.5 mg/mL while the concentration of isolated A fragment was 3 mg/mL. Tricine (50 mM) was used for scans of toxin at pH 9, 8, and 7. For other pHs the buffer was exchanged by dialyzing the sample in the desired buffer overnight at pH 7.2. The pH of the sample was adjusted at 10 °C immediately before loading 1.2 mL into the calorimeter. The buffers used were 50 mM Tricine for pH 9 and 8, 50 mM sodium phosphate for pH 7 and 6, 50 mM sodium acetate for pH 6–4, and 50 mM glycine for pH 3.

Results

Thermal Stability of Toxin. The excess heat capacity vs temperature function associated with a sample of a nicked, monomeric native mixture of nucleotide-free and -bound diphtheria toxin in 50 mM Tricine, pH 8.0, is shown in Figure 1. This calorimetric scan is characterized by a peak centered at approximately 58 °C corresponding to the thermal unfolding of the toxin molecule. Inspection of the calorimetric transition profile reveals the presence of a marked asymmetry or shoulder toward the low-temperature end of the transition. The amplitude of the shoulder was found to vary between toxin lots and was quantitatively related to the existence of variable

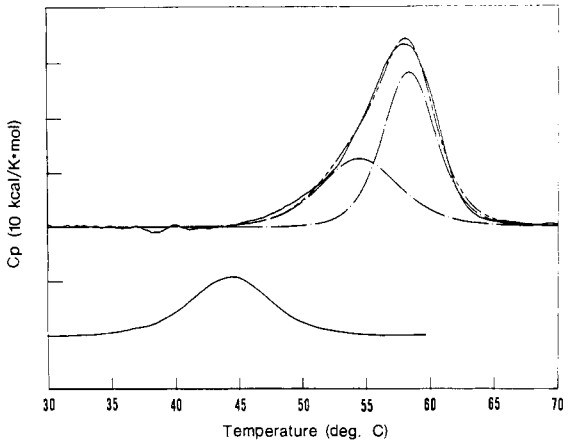

FIGURE 2: Excess heat capacity vs temperature for nucleotide-bound diphtheria toxin (upper curves) and isolated A fragment (bottom curve) at pH 8. The dashed curve is the theoretical curve calculated with the deconvolution parameters obtained for this transition (see text for details). The dotted line represents the individual contributions of the two individual transition steps to the overall curve. The dashed line is the sum of the two fitted curves. The A fragment concentration was 3.0 mg/mL.

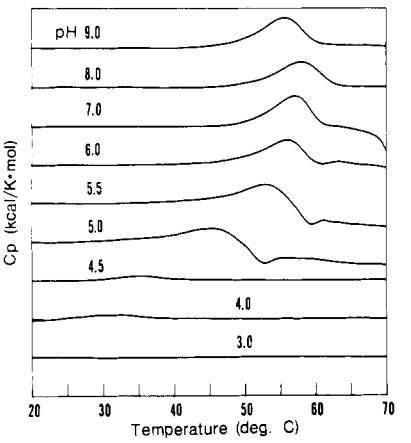

FIGURE 3: pH dependence of the excess heat capacity for nucleotide-bound diphtheria toxin in low ionic strength buffer. The buffers were 50 mM glycine, pH 3.0; 50 mM sodium acetate, pH 4.0–5.5; 50 mM phosphate, pH 6.0–7.0; and 50 mM Tricine, pH 8.0 and 9.0.

amounts of nucleotide-free and -bound species in the native toxin. Experiments with purified nucleotide-free and nucleotide-bound samples yield the calorimetric profiles shown at the bottom of Figure 1. The thermal unfolding of the nucleotide-free toxin is characterized by a transition temperature (T_m) of 51.8 °C and an enthalpy change (ΔH_{cal}) of 235 ± 20 kcal/mol while the nucleotide-bound toxin is characterized by a T_m of 58.2 °C and a ΔH_{cal} of 280 ± 20 kcal/mol. The difference of approximately 50 kcal/mol most likely reflects a combination of effects including the temperature dependence of the enthalpy change, the enthalpy associated with the release of the bound nucleotide upon thermal unfolding, and any nucleotide-induced difference in the conformation of the folded forms of the toxin. In this respect, Collins et al. (1984) have previously estimated a binding enthalpy of −28 kcal/mol for the dinucleotide ApUp from the temperature dependence of the forward- and reverse-rate binding constants. Furthermore, the binding of the nucleotide has a strong stabilizing effect as reflected by the upward shift of 6.5 °C in the transition temperature of the toxin.

The heat capacity profiles associated with the thermal unfolding of the nucleotide-free and nucleotide-bound toxins do not represent two-state transitions. In fact, the ratios of the van't Hoff to calorimetric enthalpies ($\Delta H_{VH}/\Delta H_{cal}$) are equal to 0.75 and 0.40 for the nucleotide-free and nucleotide-bound forms, respectively. A $\Delta H_{VH}/\Delta H_{cal}$ ratio smaller than unity is indicative of a multistep unfolding transition (Biltonen & Freire, 1978). Deconvolution analysis of the heat capacity data (Freire & Biltonen, 1978) followed by nonlinear least-squares optimization (Rigell et al., 1985) indicates that the overall excess heat capacity function of the toxin is composed of a minimum of two different two-state transitions as shown in Figure 2 for the nucleotide-bound toxin. The low-temperature peak is characterized by a T_m of 54.5 ± 0.1 °C and a ΔH_{cal} of 115 ± 15 kcal/mol while the high-temperature peak is characterized by a T_m of 58.4 ± 0.2 °C and a ΔH_{cal} of 164 ± 8 kcal/mol. These values correspond to entropy changes (ΔS) of 351 cal/(mol·deg) and 495 cal/(mol·deg), respectively.

On the basis of the molecular weights of fragments A and B of the toxin, the low enthalpy/low transitition temperature component was tentatively assigned to the smaller A fragment and the high enthalpy/high transition temperature component to the B fragment. In order to obtain experimental support for this assignment, calorimetric experiments were performed with the isolated A fragment. As shown in Figure 2, the excess heat capacity function associated with the isolated A fragment is highly symmetric and characterized by a T_m of 44.2 ± 0.2 °C. The calorimetric enthalpy was 89 ± 10 kcal/mol and the calculated van't Hoff enthalpy was 100 kcal/mol, which are similar to that of the low-temperature peak in the deconvoluted heat capacity profile of the intact toxin. The smaller ΔH_{cal} for the isolated A fragment is expected from the temperature dependence of the enthalpy observed for proteins of similar molecular weights (Privalov, 1979). Furthermore, the $\Delta H_{VH}/\Delta H_{cal}$ for the isolated A fragment is 1.1, indicating that this transition is closely approximated by the two-state mechanism. In this respect, the behavior of the isolated A fragment resembles that of other small globular proteins (Privalov, 1979).

The most significant conclusion from the calorimetric data for the isolated A fragment is that its transition temperature is 10 deg lower than that of the lower melting component in the intact nucleotide-bound toxin and 6.5 deg lower than that of the lower melting component in the nucleotide-free toxin. This observation is indicative of the existence of strong interfragment stabilizing interactions within the intact toxin. In fact, the B fragment is insoluble in aqueous solutions when separated from the A fragment. Furthermore, the unfolding transition of the isolated A fragment is reversible (better than 80% under our experimental conditions) whereas that of the intact toxin is not. Presumably, the irreversibility of the unfolding transition of the intact toxin is due to the hydrophobic character of the B fragment.

pH Dependence of Diphtheria Toxin Unfolding. The thermal unfolding of the intact, cytoxically active, nicked, monomeric nucleotide-bound diphtheria toxin is strongly dependent on pH. As indicated in Figure 3, the toxin is most stable in the neutral to slightly alkaline pH range. At acidic pHs, however, the native conformation of the protein shows a large decrease in stability expressed as both an abrupt reduction in the transition temperature and the transition enthalpy below pH 5. These changes define very sharp sigmoidal profiles centered at approximately pH 5.0 at low salt concentrations and pH 5.5 at 0.2 M NaCl as shown in Figure 4. The pH location and salt dependence of the diphtheria toxin transition measured calorimetrically are in excellent agreement with the fluorescence and circular dichroism measurements of Blewitt et al. (1985). These authors also concluded that below the pH transition and at 21–23 °C the toxin was not

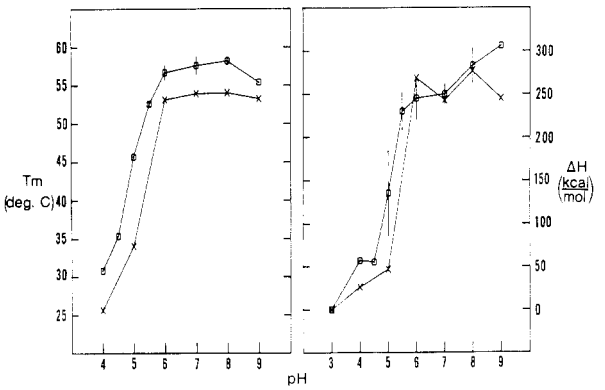

FIGURE 4: pH dependence of the T_m and enthalpy of unfolding for nucleotide-bound toxin. The conditions for high ionic strength buffers (0.2 M NaCl) are the same as for low ionic strength buffers, except that Tricine buffer was used instead of phosphate buffer at pH 6–7. The error bars are for experiments in which more than one protein preparation was used. (○) represents low ionic strength buffers, and (×) represents high ionic strength buffers.

completely unfolded into a random coil and had some residual structure. This is consistent with the calorimetric data (see for example calorimetric scan at pH 4 in Figure 3) which report a residual unfolding process at low pH.

At pHs ranging between 7 and 5 the thermal unfolding of the toxin is followed by protein precipitation that results in the appearance of exothermic heat effects in the heat capacity profile (see Figure 3). Under these circumstances it is difficult to calculate the enthalpy changes by direct integration of the excess heat capacity function. In those cases, the total enthalpy was estimated by extrapolation of the partial enthalpy observed up to the temperature of the maximum in the heat capacity function. This extrapolation was done semiempirically after noticing that for all experiments in which postdenaturational precipitation did not occur the partial enthalpy up to the temperature of the maximum in the excess heat capacity function was 0.63 ± 0.03 of the total. When the calorimetric enthalpy change is plotted against the transition temperature for pH ≥ 5, a ΔC_p of 0.19 cal/(deg·g) is obtained. Values ranging between 0.09 and 0.16 cal/(deg·g) have previously been observed for small (M_r < 20000) water-soluble proteins (Privalov, 1979). The higher value observed for diphtheria toxin is consistent with a higher proportion of hydrophobic contacts in this protein (Privalov, 1979) and also consistent with the ability of this protein to insert into the hydrophobic core of the membrane upon unfolding. It seems that the insertion mechanism of diphtheria toxin is built around the intrinsic thermodynamic properties of this protein.

pH/Temperature Stability Diagram. The calorimetric results presented above allow calculation of the *apparent* fraction of molecules in the unfolded state or fractional degree of unfolding (P_u) as a function of pH at any temperature. This is done by calculating the normalized partial enthalpy up to a preselected temperature and plotting it as a function of pH. The pH stability isotherms are illustrated in Figure 5 for the experiments at low ionic strength (upper panel) and the experiments in the presence of 0.2 M NaCl (lower panel). Figure 5 allows calculation of the fractional degree of unfolding at different temperatures for any given pH. Since in aqueous solutions the B subunit precipitates upon unfolding due to its, hydrophobic character, this diagram should be read in the unfolding direction only. This figure indicates that at physiological temperature (37 °C) the midpoint of the pH-induced unfolding occurs at pH 4.7 at low ionic strength and at pH 5.4 in the presence of 0.2 M NaCl. These results provide support for the proposal that endosomal acidification provides

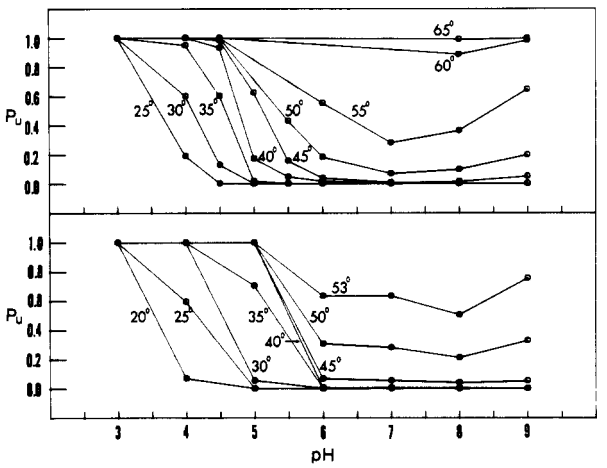

FIGURE 5: pH/temperature stability diagram for nucleotide-bound toxin. The various curves represent the fractional degree of unfolding as a function of pH for the indicated temperatures. The upper panel is for low ionic strength buffer while the lower panel is for high ionic strength buffer.

the driving force for the toxin structural transformation preceding membrane insertion.

Discussion

Nicked diphtheria toxin consists of two fragments joined by a disulfide bridge. The two fragments are stabilized by a combination of intrafragment and interfragment interactions. This conclusion is illustrated by different calorimetric observations. First, there is a 6.5 °C difference in the transition temperatures of the A fragment free in solution and attached to the B fragment. This transition temperature difference represents a change of −2.6 kcal/mol in the free energy of stabilization of the A fragment as estimated with the van't Hoff equation. Second, the B fragment is hydrophobic and precipitates from solution when separated from the A fragment. The attachment of the A fragment makes the B fragment and consequently the entire toxin molecule soluble in aqueous solutions at neutral pH. Third, the unfolding mechanism of the entire toxin involves a minimum of two transition steps as deduced from the deconvolution of the excess heat capacity function (Freire & Biltonen, 1978). These transitions are not independent of each other as would be the case for a multidomain protein stabilized primarily by intradomain interactions. Even though at this point structural information only exist at 3-Å resolution for a diphtheria toxin dimer (Kantardjieff et al., 1987), it is worth noticing that the crystallographic data indicate the existence of at least two domains in the diphtheria toxin monomers.

From the point of view of the membrane insertion and translocation mechanism of the toxin, the most important observations are those related to the pH-induced transition. Previous spectroscopic studies (Blewitt et al., 1984) have reported the existence of a conformational change centered around pH 5. The calorimetric results confirm those studies and furthermore indicate that this is a massive unfolding of the toxin molecule as indicated by the magnitude of the enthalpy change for this process. Approximately 85% of the total enthalpy of unfolding is absorbed in passing the toxin sample from pH 7 to 4. This unfolding process exposes hydrophobic residues and presumably provides the driving force for membrane insertion. It should be noted that recent studies using intact cells (Johnson et al., 1988) suggest that the membrane insertion of the toxin does not require a specific receptor. Apparently, the receptor provides a binding site that places

the toxin in close proximity to the membrane but does not play a specific role in the insertion process. Within this context, insertion would be a thermodynamically favorable process once the toxin has undergone its pH-induced transition. After the toxin penetrates the endosomal membrane, the A fragment is translocated to the cystosolic side and exposed again to a neutral pH. This exposure of the A fragment to a neutral pH should trigger its refolding as indicated by the calorimetric observation that the A fragment unfolding transition is a reversible process.

The binding of dinucleotides, primarily ApUp, stabilizes the entire toxin molecule, as shown by the higher T_m observed for nucleotide-bound diphtheria toxin. This stabilization involves the entire toxin molecule and not only one of the toxin fragments as shown in the heat capacity profiles for the nucleotide-free and -bound toxin (Figure 1). The low- and high-temperature components of the transition are shifted to higher temperatures, showing that all domains of the toxin are at least in part stabilized by nucleotide binding. This picture is consistent with the model given by Lory et al. (1980) in which the 3′-phosphate of the dinucleotide interacts with the P site on the B fragment and the adenylyl-3′,5′-uridine binds to the NAD^+ site on the A fragment.

The most notable difference in the behavior of diphtheria toxin at different ionic strengths is the 5 °C downward shift in T_m observed at high salt concentration. Increasing the ionic strength would have the effect of disrupting salt bridges which would result in the destabilization of the native conformation. This is also consistent with the observation that at any given T_m the calorimetric enthalpies are independent of salt concentration within the experimental error for the salt concentrations studied. The formation of salt bridges is primarily driven by entropic forces (Schulz & Schirmer, 1979), which would account for the absence of a noticeable enthalpic effect by salt.

The pH/temperature stability diagram (Figure 5) shows that at any temperature the toxin is most stable at pH 7–8. As the pH departs from neutrality, the temperature-induced unfolding begins at progressively lower temperatures, until at pH 3 the toxin is unfolded at all temperatures. It can also be seen that at 37 °C a change in the pH from 5.5 to 4.5 shifts the fraction of unfolded toxin from 0.01 to 0.80 and that increasing the ionic strength increases the pH sensitivity. These observations show that the conditions found within a prelysosomal endosome (Jensen & Bainton, 1973) would be sufficient to induce the unfolding of diphtheria toxin.

pH-induced protein conformational transitions appear to provide a widespread mechanism directed to facilitate or trigger the onset of hydrophobic interactions in protein–membrane systems. These interactions might result in protein insertion like in the case of diphtheria toxin or in membrane fusion like in the case of some viral fusion proteins (Mellman et al., 1986). The results presented in this paper and studies currently under way in this laboratory are aimed at elucidating the energetics and thermodynamic mechanism of these processes.

References

Biltonen, R. L., & Freire, E. (1978) *CRC Crit. Rev. Biochem. 5*, 85–124.

Blewitt, M. G., Zhao, J. J., McKeever, B., Sarma, R., & London, E. (1984) *Biochem. Biophys. Res. Commun. 120*, 286–290.

Blewitt, M. G., Chung, L. A., & London, E. (1985) *Biochemistry 24*, 5458–5464.

Cieplak, W., Gaudin, H. M., & Eidels, L. (1987) *J. Biol. Chem. 262*, 13246–13253.

Collier, R. J., & Kandel, J. (1971) *J. Biol. Chem. 246*, 1496–1503.

Collins, C. M., Barbieri, J. T., & Collier, R. J. (1984) *J. Biol. Chem. 259*, 15154–15158.

DeLange, R. J., Williams, L. C., & Collier, R. J. (1979) *J. Biol. Chem. 254*, 5827–5831.

Donovan, J. J., Simon, M. I., & Montal, M. (1985) *J. Biol. Chem. 260*, 8817–8823.

Draper, R. K., & Simon, M. I. (1980) *J. Cell Biol. 87*, 849–854.

Drazin, R. E., Collier, R. J., Williams, L. C., & DeLange, R. J. (1979) *J. Biol. Chem. 254*, 5832–5837.

Falmagne, P., Capiau, C., Lambotte, P., Zanen, J., Cabiaux, V., & Ruysschaert, J. M. (1985) *Biochim. Biophys. Acta 827*, 45–50.

Freire, E., & Biltonen, R. L. (1978) *Biopolymers 17*, 463–479.

Gill, D. M., & Steinhaus, D. M. (1974) *J. Hyg., Epidemiol., Microbiol., Immunol. 18*, 316–323.

Goor, R. S. (1968) *Nature (London) 217*, 1051–1053.

Hranitzky, K. W., Durham, D. L., Hart, D. A., & Eidels, L. (1985) *Infect. Immun. 49*, 336–343.

Jensen, M. S., & Bainton, D. F. (1973) *J. Cell. Biol. 56*, 379–388.

Johnson, V. G., Wilson, D., Greenfield, L., & Youle, R. J. (1988) *J. Biol. Chem. 263*, 1295–1300.

Kandel, J., Collier, R. J., & Chung, D. W. (1980) *J. Biol. Chem. 249*, 2088–2097.

Kantardjieff, K., Dijkstra, B., Westbrook, E. M., Barbieri, J. T., Carrol, S. F., Collier, R. J., & Eisenberg, D. (1987) *UCLA Symp. Mol. Cell. Biol., New Ser. 69*, 187–200.

Lory, S., Carroll, S. F., & Collier, R. J. (1980) *J. Biol. Chem. 255*, 12016–12019.

Lowry, O. H., Rosebrough, N. J., Farr, A. L., & Randell, R. J. (1951) *J. Biol. Chem. 193*, 265–275.

Marnell, M. H., Shia, S. P., Stookey, M., & Draper, R. K. (1984) *Infect. Immun. 44*, 145–150.

Mellman, I., Renate, F., & Helenius, A. (1986) *Annu. Rev. Biochem. 55*, 663–700.

Moskaug, J. O., Sandvig, K., & Olsnes, S. (1987) *J. Biol. Chem. 262*, 10339–10345.

Ohkuma, S., & Poole, B. (1978) *Proc. Natl. Acad. Sci. U.S.A. 75*, 3327–3331.

Privalov, P. L. (1979) *Adv. Protein Chem. 33*, 167–241.

Proia, R. L., Hart, D. A., Holmes, R. K., Holmes, K. V., & Eidels, L. (1979) *Proc. Natl. Acad. Sci. U.S.A. 76*, 685–689.

Rigell, C., deSaussure, C., & Freire, E. (1985) *Biochemistry 24*, 5638–5646.

Sandvig, K., & Olsnes, S. (1980) *J. Cell. Biol. 87*, 828–832.

Sandvig, K., & Olsnes, S. (1981) *J. Biol. Chem. 256*, 9068–9076.

Sandvig, K., & Olsnes, S. (1982) *J. Biol. Chem. 257*, 7495–7503.

Schulz, G. E., & Schirmer, R. H. (1979) in *Principles of Protein Structure* (Canton, C. R., Ed.) p 41, Springer-Verlag, New York.